

This article was downloaded by:

On: 23 January 2011

Access details: *Access Details: Free Access*

Publisher *Taylor & Francis*

Informa Ltd Registered in England and Wales Registered Number: 1072954 Registered office: Mortimer House, 37-41 Mortimer Street, London W1T 3JH, UK



## Journal of Coordination Chemistry

Publication details, including instructions for authors and subscription information:

<http://www.informaworld.com/smpp/title~content=t713455674>

### Synthesis, characterization, antimicrobial, and nuclease activity studies of some metal Schiff-base complexes

D. Arish<sup>a</sup>; M. Sivasankaran Nair<sup>a</sup>

<sup>a</sup> Department of Chemistry, Manonmaniam Sundaranar University, Tirunelveli-627012, Tamil Nadu, India

First published on: 13 May 2010

**To cite this Article** Arish, D. and Sivasankaran Nair, M.(2010) 'Synthesis, characterization, antimicrobial, and nuclease activity studies of some metal Schiff-base complexes', *Journal of Coordination Chemistry*, 63: 9, 1619 – 1628, First published on: 13 May 2010 (iFirst)

**To link to this Article:** DOI: 10.1080/00958972.2010.483729

**URL:** <http://dx.doi.org/10.1080/00958972.2010.483729>

PLEASE SCROLL DOWN FOR ARTICLE

Full terms and conditions of use: <http://www.informaworld.com/terms-and-conditions-of-access.pdf>

This article may be used for research, teaching and private study purposes. Any substantial or systematic reproduction, re-distribution, re-selling, loan or sub-licensing, systematic supply or distribution in any form to anyone is expressly forbidden.

The publisher does not give any warranty express or implied or make any representation that the contents will be complete or accurate or up to date. The accuracy of any instructions, formulae and drug doses should be independently verified with primary sources. The publisher shall not be liable for any loss, actions, claims, proceedings, demand or costs or damages whatsoever or howsoever caused arising directly or indirectly in connection with or arising out of the use of this material.

## Synthesis, characterization, antimicrobial, and nuclease activity studies of some metal Schiff-base complexes

D. ARISH and M. SIVASANKARAN NAIR\*

Department of Chemistry, Manonmaniam Sundaranar University,  
Tirunelveli – 627012, Tamil Nadu, India

(Received 30 July 2009; in final form 22 January 2010)

A Schiff base (L) is prepared by condensation of cuminaldehyde and L-histidine, and characterized by elemental analysis, IR, UV-Vis,  $^1\text{H-NMR}$ ,  $^{13}\text{C-NMR}$ , and mass spectra. Co(II), Ni(II), Cu(II), and Zn(II) complexes of this Schiff-base ligand are synthesized and characterized by elemental analysis, molar conductance, mass, IR, electronic spectra, magnetic moment, electron spin resonance (ESR), CV, TG/DTA, powder XRD, and SEM. The conductance data indicate that all the complexes are 1:1 electrolytes. IR data reveal that the Schiff base is a tridentate monobasic donor, coordinating through azomethine nitrogen, imidazole nitrogen, and carboxylato oxygen. The electronic spectral data and magnetic measurements suggest that Co(II) and Ni(II) complexes are tetrahedral, while Cu(II) complex has distorted square planar geometry. XRD and SEM show that Co(II), Cu(II), and Zn(II) complexes have crystalline nature, while the Ni(II) complex is amorphous and the particles are in nanocrystalline phase. The *in vitro* biological activities of the synthesized compounds were tested against the bacterial species, *Escherichia coli*, *Bacillus subtilis*, *Pseudomonas aeruginosa*, and *Staphylococcus aureus*; and fungal species, *Aspergillus niger*, *Aspergillus flavus*, and *Candida albicans* by the disc diffusion method. The biological study indicates that complexes exhibit more activity than the ligand. The nuclease activity of the ligand and its complexes are assayed on CT DNA using gel electrophoresis in the presence and the absence of  $\text{H}_2\text{O}_2$ . The Cu(II) complex shows increased nuclease activity in the presence of an oxidant when compared to the ligand, Co(II) and Ni(II) complexes.

**Keywords:** Schiff base; IR; Electronic; ESR; Antimicrobial activity

### 1. Introduction

Considerable attention has been given to transition metal complexes of Schiff bases derived from amino acids because of their unusual configurations and biological importance [1–5]. Amino acid Schiff bases are active against a wide range of organisms, playing an important role in decarboxylation, transamination, and C–C bond cleavage [6, 7]. The interaction of metal complexes with DNA has gained much attention due to possible applications such as new therapeutic agents [8]. Among the amino acids, L-histidine is present in many copper enzymes and proteins [9]. Recently, we studied Co(II), Ni(II), Cu(II), and Zn(II) complexes of a Schiff base involving furfural and L-histidine and their antibacterial activity toward *Escherichia coli* and

\*Corresponding author. Email: msnairchem@rediffmail.com

*Staphylococcus aureus* [10]. Cuminaldehyde (*p*-isopropylbenzaldehyde) is a biologically important aromatic aldehyde [11–13] used as perfumes, food flavors, and other cosmetics. However, only a few transition metal complexes of cuminaldehyde Schiff base have been reported [14–17]. This article reports some new Co(II), Ni(II), Cu(II), and Zn(II) complexes of Schiff base derived from cuminaldehyde and L-histidine.

## 2. Experimental

### 2.1. Materials

L-Histidine was purchased from Sigma and used without purification. Cuminaldehyde was obtained from Himedia and CT DNA from Genei, Bangalore. The samples Co(II), Ni(II), Cu(II), and Zn(II) chlorides were obtained from Merck. All other reagents and solvents were purchased from commercial sources at analytical grades.

### 2.2. Synthesis of Schiff-base ligand

L-Histidine (0.776 g, 5 mmol) was dissolved in 20 mL of MeOH containing KOH (0.28 g, 5 mmol). A solution of cuminaldehyde (0.741 g, 5 mmol) in 20 mL of absolute MeOH was added dropwise with stirring and refluxed at 50 °C for 8 h. The volume of the yellow solution was reduced *in vacuo* using a rotary evaporator. Anhydrous ether was added to obtain a yellowish precipitate, which was then recrystallized from MeOH. The purity of the Schiff base was checked by TLC.

### 2.3. Synthesis of the Schiff-base metal(II) complexes

A solution of metal(II) chloride in 20 mL of aqueous MeOH (5 mmol) was added dropwise to the yellowish solution of Schiff base in 20 mL of MeOH (5 mmol) with constant stirring. The reaction mixture was heated under reflux for 2 h and the volume was reduced to half of the initial volume under reduced pressure. The precipitate was filtered-off, washed several times with cold EtOH and ether, and then dried *in vacuo* over anhydrous CaCl<sub>2</sub>.

### 2.4. Physical measurements

Elemental analysis was done using a Perkin Elmer elemental analyzer. The mass spectra of the Schiff-base ligand and its complexes were recorded on a JEOL SX 102/DA-600 mass spectrometer. The <sup>1</sup>H and <sup>13</sup>C-NMR spectra of the Schiff base were recorded on a JEOL GSX 400 FT-NMR spectrometer. The metal contents in the complexes were determined by standard EDTA titration [18]. Molar conductances of the complexes were measured in MeOH (10<sup>-3</sup> mol L<sup>-1</sup>) solutions using a coronation digital conductivity meter. IR spectra were recorded in KBr discs on a JASCO FT/IR-410 spectrometer from 4000 to 400 cm<sup>-1</sup>. Electronic spectra were recorded on a Perkin Elmer Lambda-25 UV-Vis spectrometer. Room temperature magnetic measurements were performed on a Guoy balance making diamagnetic corrections using Pascal's constants. The X-band

electron spin resonance (ESR) spectrum of Cu(II) complex was recorded on a Varian E112 X-band spectrometer. Cyclic voltammetric measurements were carried out in a bio-analytical system (BAS) model CV-50 W electrochemical analyzer. The three-electrode cell comprised of a reference Ag/AgCl, auxiliary platinum, and working glassy electrodes. Tetrabutylammonium perchlorate was used as the supporting electrolyte. Thermal analysis was carried out on a SDT Q 600/V8.3 build 101 thermal analyzer with a heating rate of  $20^{\circ}\text{C min}^{-1}$  using  $\text{N}_2$ . Powder XRD was recorded on a Rigaku Dmax X-ray diffractometer with Cu-K $\alpha$  radiation. SEM images were recorded in a Hitachi SEM analyzer.

### 2.5. Antimicrobial activities

Antibacterial and antifungal activities of the ligand and its complexes were tested *in vitro* against bacteria *E. coli* (MSU B01), *Bacillus subtilis* (MSU B02), *Pseudomonas aeruginosa* (MSU B03) and *S. aureus* (MSU B04); and fungi *Aspergillus niger* (MSU F01), *Aspergillus flavus* (MSU F02), and *Candida albicans* (MSU F03) by the disc diffusion method [19]. *Amikacin*, *Ofloxacin*, and *Ciprofloxacin* were used as standards for antibacterial activity and *Nystatin* was used as standard for antifungal activity. The test organisms were grown on nutrient agar medium in petri plates. The compounds were prepared in dimethyl sulfoxide (DMSO) and soaked in filter paper discs, each of 5 mm diameter and 1 mm thickness. The discs were placed on the previously seeded plates and incubated at  $37^{\circ}\text{C}$ ; the diameter of inhibition zone around each disc was measured after 24 h for antibacterial and 72 h for antifungal activities.

### 2.6. Gel electrophoresis

A solution of CT DNA in  $0.5\text{ mmol L}^{-1}$  NaCl/ $5\text{ mmol L}^{-1}$  tris-HCl (pH 7.0) gave a ratio of UV absorbance in the range 1.8–1.9 at 260 and 280 nm ( $A_{260}/A_{280}$ ), indicating that the DNA was sufficiently free of proteins [17]. Cleavage reactions were run between the metal complexes and DNA, and the solutions were diluted with loading dye using 1% agarose gel. Then  $3\text{ }\mu\text{L}$  of ethidium bromide ( $0.5\text{ }\mu\text{g mL}^{-1}$ ) was added to the above solution and mixed well. The warmed agarose was poured and clamped immediately with a comb to form sample wells. The gel was mounted into an electrophoretic tank and enough electrophoretic buffers were added to cover the gel to a depth of about 1 mm. The DNA sample ( $30\text{ }\mu\text{mol L}^{-1}$ ),  $50\text{ }\mu\text{mol L}^{-1}$  metal complex, and  $500\text{ }\mu\text{mol L}^{-1}$   $\text{H}_2\text{O}_2$  in  $50\text{ mmol L}^{-1}$  tris-HCl buffer (pH 7.1) were mixed with loading dye and loaded into the well of the submerged gel using a micropipette. Electric current (50 mA) was passed into running buffer. After 1–2 h, the gel was taken from the buffer. After electrophoresis, the gel was photographed under UV transilluminator (280 nm) and documented.

## 3. Results and discussion

### 3.1. Characterization of Schiff-base ligand

The results of the elemental analysis (table 1) of the Schiff base are in good agreement with those calculated for the suggested formula. The mass spectrum shows a

Table 1. Analytical and physical data of the Schiff base and its complexes.

Compound	Empirical formula	Color	Elemental analysis				Molar conductance ( $\Omega^{-1} \text{cm}^2 \text{mol}^{-1}$ )
			Found (Calcd) %				
			C	H	N	M	
L	$\text{KC}_{16}\text{H}_{18}\text{N}_3\text{O}_2$	Yellow	58.72 (59.42)	4.89 (5.61)	13.08 (12.99)	–	–
$[\text{CoL}(\text{H}_2\text{O})]\text{Cl}$	$\text{CoC}_{16}\text{H}_{20}\text{N}_3\text{O}_3\text{Cl}$	Violet	48.96 (48.44)	4.97 (5.08)	11.04 (10.59)	15.11 (14.85)	85
$[\text{NiL}(\text{H}_2\text{O})]\text{Cl}$	$\text{NiC}_{16}\text{H}_{20}\text{N}_3\text{O}_3\text{Cl}$	Pale green	48.92 (48.47)	5.01 (5.08)	10.95 (10.60)	15.03 (14.80)	80
$[\text{CuL}(\text{H}_2\text{O})]\text{Cl}$	$\text{CuC}_{16}\text{H}_{20}\text{N}_3\text{O}_3\text{Cl}$	Blue	47.22 (47.88)	4.85 (5.02)	10.92 (10.47)	15.23 (15.83)	85
$[\text{ZnL}(\text{H}_2\text{O})]\text{Cl}$	$\text{ZnC}_{16}\text{H}_{20}\text{N}_3\text{O}_3\text{Cl}$	Yellow	48.09 (47.66)	4.73 (5.00)	9.97 (10.42)	16.04 (16.22)	83

well-defined molecular ion peak at  $m/z = 323$  (relative intensity = 14%), which coincides with the formula weight of the Schiff base.

$^1\text{H}$ - and  $^{13}\text{C}$ -NMR spectra of the Schiff base are given in Supplementary material. In the  $^1\text{H}$ -NMR spectrum, azomethine proton gives a singlet at 8.35 ppm and the aromatic and imidazole ring protons appear at 7.2–7.9 ppm. The imidazole N–H gives the peak at 13.2 ppm. In the  $^{13}\text{C}$ -NMR spectrum, the azomethine carbon and the carboxylato carbons are at 172 and 179 ppm, respectively. The IR spectrum of the Schiff base exhibits a broad band centered at  $1585 \text{cm}^{-1}$  due to azomethine group  $\nu(\text{C}=\text{N})$ , which overlaps with the asymmetric carboxylato stretching modes (Supplementary material). This value is comparable with that of cuminaldehyde thiosemicarbazone [14–17]. The bands are probably broadened because of overlap with aromatic ring carbon stretching and imidazole ring imido nitrogen-stretching frequencies [20, 21]. In the electronic spectrum of the ligand, the band at 304 nm is attributed to  $\pi$ – $\pi^*$  transition of the azomethine ( $>\text{C}=\text{N}$ ) chromophore. The intense absorption at higher energy, 270 nm, is presumably from the  $\pi$ – $\pi^*$  transition of the benzene ring of the Schiff base. The 3-D structure of the Schiff-base ligand has been obtained using MOPAC [22], shown in Supplementary material.

### 3.2. Characterization of metal Schiff-base complexes

Analytical and physical characterizations of the Schiff-base complexes are given in table 1. The analytical data show that the metal-to-ligand ratio is 1:1. The composition of the complexes is  $[\text{ML}(\text{H}_2\text{O})]\text{Cl}$ , where L is the Schiff-base ligand. The Co(II), Ni(II), and Cu(II) complexes are soluble in MeOH, dimethylformamide (DMF), and DMSO but insoluble in other common organic solvents, and Zn(II) complex is slightly soluble in MeOH and DMSO. The low solubility of Zn(II) complex in common organic solvents hinders its study in solution. The mass spectra of the Co(II), Ni(II), Cu(II), and Zn(II) complexes show a molecular ion peak at  $m/z$  (relative intensity) = 397 (18%), 396 (38%), 401 (45%), and 403 (12%), respectively, which coincides with the formula weight of the Schiff-base complexes.

The high molar conductance (table 1) values of  $10^{-3} \text{mol L}^{-1}$  solution in MeOH show that all the complexes are 1:1 electrolytes [23]. The presence of uncoordinated chloride is also confirmed by silver nitrate test [18].

Table 2. IR spectral data of ligand and its complexes ( $\text{cm}^{-1}$ ).

Compound	$\nu_{\text{azo}}(\text{C}=\text{N}), \nu_{\text{asym}}(\text{COO}^-)$ $\nu_{\text{imida ring}}(\text{C}=\text{N})$	$\nu_{\text{sym}}(\text{COO}^-)$	$\nu(\text{H}_2\text{O})$	$\nu(\text{M}-\text{O})$	$\nu(\text{M}-\text{N})$
L	1585	1400	3350	—	—
[CoL(H <sub>2</sub> O)]Cl	1602	1395	3358	510	432
[NiL(H <sub>2</sub> O)]Cl	1605	1393	3360	515	420
[CuL(H <sub>2</sub> O)]Cl	1615	1393	3355	520	450
[ZnL(H <sub>2</sub> O)]Cl	1607	1394	3360	517	425

Table 3. Electronic and magnetic moment data of metal complexes.

Compound	Electronic spectra wavelength (nm)	Magnetic moment (BM)	Geometry
L	270,304	—	—
[CoL(H <sub>2</sub> O)]Cl	560	4.21	Tetrahedral
[NiL(H <sub>2</sub> O)]Cl	610	3.32	Tetrahedral
[CuL(H <sub>2</sub> O)]Cl	650	1.83	Distorted square planar

### 3.3. IR spectra

IR spectral data are given in table 2. On complexation, the band at  $1585\text{ cm}^{-1}$  for the azomethine shifted to higher frequency at  $\sim 1600\text{--}1615\text{ cm}^{-1}$  in the metal complexes indicating coordination of the azomethine nitrogen to the metal ion [14]. For the free ligand the band at  $1400\text{ cm}^{-1}$  can be ascribed to  $\nu_{\text{s}}(\text{COO}^-)$  group. During complexation, this shifts to a lower frequency by *ca*  $5\text{--}7\text{ cm}^{-1}$ , indicating coordination between metal ion and carboxylato oxygen. The difference between  $\nu_{\text{as}}(\text{COO}^-)$  and  $\nu_{\text{s}}(\text{COO}^-)$  is  $\sim 200\text{ cm}^{-1}$ , indicating monodentate binding of carboxylato [21, 24]. The presence of coordinated water in the complexes is indicated by the very broad absorption centered at  $\sim 3360\text{ cm}^{-1}$  (table 2) [25]. In the lower frequency region, weak bands at  $510\text{--}520$  and  $420\text{--}450\text{ cm}^{-1}$  have been assigned to the  $\nu(\text{M}-\text{O})$  and  $\nu(\text{M}-\text{N})$  vibrations, respectively.

### 3.4. Electronic spectra

The electronic spectrum of tetrahedral Co(II) complexes is reported to have only one absorption in the visible region due to  ${}^4\text{A}_2(\text{F}) \rightarrow {}^4\text{T}_1(\text{P})$  transition [26]. The present Co(II) complex (table 3) has one band in the visible region at 560 nm, indicating tetrahedral geometry. The spectrum of the Ni(II) complex shows an intense absorption at 610 nm [26], due to the  ${}^3\text{T}_1(\text{F}) \rightarrow {}^3\text{T}_1(\text{P})$  transition for tetrahedral geometry. The Cu(II) complex exhibits a broad band centered at 650 nm, which can be assigned to  ${}^2\text{B}_{1\text{g}} \rightarrow {}^2\text{B}_{2\text{g}}$  transition corresponding to a square planar environment around Cu(II). The weak band at  $\sim 1000\text{ nm}$  in the complexes can be attributed to a bigger distortion in molecular geometry from square planar to tetrahedral geometry [27], that is the imidazole nitrogen tends to move apart from planarity [28].

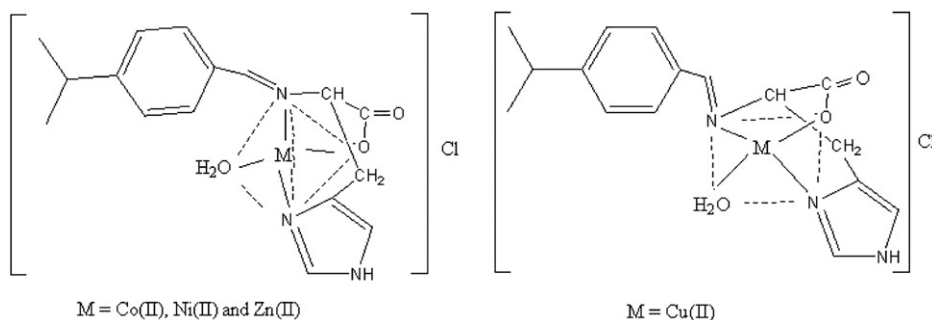


Figure 1. Proposed structure of the complexes.

### 3.5. Magnetic properties

The magnetic moment data of the complexes are given in table 3. Tetrahedral Co(II) with a  $^4A_2$  ground state has been reported to have magnetic moments in the range 4.2–4.8 BM [29]. The present Co(II) complex has a magnetic moment of 4.21 BM. Generally, square planar Ni(II) complexes are diamagnetic while tetrahedral complexes have moments in the range 3.2–4.1 BM [30]. The Ni(II) complex reported herein has a room temperature magnetic moment of 3.32 BM, which is in the normal range for tetrahedral Ni(II). The Cu(II) complex exhibits room temperature magnetic moment of 1.83 BM, which is the value expected for a  $d^9$  metal ion in a magnetically dilute environment [31]. The electronic and magnetic studies indicate that Co(II) and Ni(II) complexes have tetrahedral geometry, while Cu(II) complex has distorted square planar geometry. The proposed structures of the complexes are given in figure 1.

### 3.6. Electrochemical studies

The cyclic voltammogram of metal(II) complexes were recorded in MeOH at 300 K in the potential range 0–1.5 V at a scan rate of  $100 \text{ mVs}^{-1}$ . The cyclic voltammogram of Cu(II) complex is shown in Supplementary material. The Co(II) complex shows an irreversible peak at  $-1.05 \text{ V}$  corresponding to ligand reduction. The irreversible ligand reduction peak was observed at  $-1.03 \text{ V}$  for the Ni(II) complex. The Cu(II) complex shows an irreversible peak at  $-1.06 \text{ V}$ , which can be tentatively assigned to the reduction of coordinated ligand.

### 3.7. Electron spin resonance

The ESR spectrum of the Cu(II) complex is recorded in DMSO at liquid nitrogen temperature (Supplementary material). Kivelson and Neiman [32] have reported  $g_{\parallel} < 2.3$  for covalent character and  $> 2.3$  for ionic character of the metal–ligand bond in complexes. For the present Cu(II) complex, the  $g_{\parallel}$  value is  $< 2.3$  and  $g_{av}$  value is  $> 2$ , indicating significant covalent character in the metal–ligand bond [33]. The observed value of 0.77 for the bonding parameter  $\alpha^2$  also indicates that the Cu(II) complex has covalent character. The trend  $g_{\parallel} (2.26) > g_{\perp} (2.04) > g_e (2.0023)$  reveals that the unpaired electron lies predominantly in  $d_{x^2-y^2}$  characteristic of distorted square planar geometry in

Table 4. Thermogravimetric data of Co(II), Ni(II), Cu(II), and Zn(II) complexes.

Complex	Temperature (°C)	DTA peak (°C)	Percentage weight loss Obs. (Calcd)	Process
[CoL(H <sub>2</sub> O)]Cl	210–230	265 Endo	4.61 (4.53)	Loss of coordinated water molecule
	250–270	350 Endo	8.78 (8.94)	Loss of chloride ion
	400–550	540 Exo	67.21 (67.63)	Loss of organic moieties
	>550	620 Exo	Residue 19.40 (18.88)	CoO
[NiL(H <sub>2</sub> O)]Cl	208–227	262 Endo	4.68 (4.54)	Loss of coordinated water molecule
	252–270	350 Endo	8.67 (8.95)	Loss of chloride ion
	410–553	550 Exo	67.71 (67.67)	Loss of organic moieties
	>553	625 Exo	Residue 18.94 (18.84)	NiO
[CuL(H <sub>2</sub> O)]Cl	214–230	260 Endo	4.56 (4.45)	Loss of coordinated water molecule
	251–272	354 Endo	8.78 (8.84)	Loss of chloride ion
	405–550	565 Exo	66.57 (66.89)	Loss of organic moieties
	>550	627 Exo	Residue 20.09 (19.82)	CuO
[ZnL(H <sub>2</sub> O)]Cl	210–268	265 Endo	4.52 (4.46)	Loss of coordinated water molecule
	252–274	351 Endo	8.72 (8.80)	Loss of chloride ion
	402–560	558 Exo	66.45 (66.61)	Loss of organic moieties
	>560	632 Exo	Residue 20.31 (20.18)	ZnO

Cu(II) complexes [34]. The empirical factor, “*f*”, an index of tetragonal distortion value of the complex is found to be 152 cm, indicating significant distortion from planarity [27].

According to Hathaway [35], if exchange interaction coupling constant,  $G > 4$ , the exchange interaction is negligible, but  $G < 4$  indicates considerable exchange interaction. In the present Cu(II) complex, the “*G*” value is  $> 4$ , indicating no interaction in the complex. Moreover, the absence of a half field signal at 1600 G corresponding to  $\Delta M = \pm 2$  transitions indicates the absence of any Cu–Cu interaction in the complex [36]. Again, the trend of orbital reduction parameters  $K_{\parallel}$  and  $K_{\perp}$  indicates  $K_{\parallel} \approx K_{\perp} \approx 0.77$  for pure  $\sigma$ -bonding,  $K_{\parallel} < K_{\perp}$  for in-plane  $\pi$  bonding and  $K_{\parallel} > K_{\perp}$  for out-of-plane  $\pi$ -bonding [35]. The observed  $K_{\parallel}(0.59) > K_{\perp}(0.17)$  demonstrates the significant contribution from out-of-plane  $\pi$ -bonding in metal–ligand bonding.

### 3.8. Thermogravimetric studies

Thermogravimetric studies have been made in the temperature range 25–900°C (Supplementary material); thermal stability data of the complexes are listed in table 4. Thermal decomposition curves of the complexes show a similar sequence of three decomposition steps. In the first step, all the complexes lost one molecule of coordinated water between 210 and 230°C, then the second step is removal of chloride as HCl gas in the 230–270°C range. The third step (380–700°C) corresponds to removal of organic ligand leaving metal oxide as residue. Differential thermal analyses of the complexes have similar properties, loss of water molecule and chloride ion as HCl are endothermic whereas removal of organic moiety and formation of metal oxide are exothermic.

### 3.9. Powder XRD

Powder XRD of Co(II), Ni(II), Cu(II), and Zn(II) complexes were recorded over the  $2\theta = 0$ –80 range and are shown in Supplementary material. From the data,



Table 5. Antibacterial and antifungal activity of the Schiff base and its complexes.

Compound	Bacterial species				Fungal species		
	<i>E. coli</i>	<i>B. subtilis</i>	<i>P. aeruginosa</i>	<i>S. aureus</i>	<i>A. niger</i>	<i>A. flavus</i>	<i>C. albicans</i>
L	+	–	–	+	+	–	+
[CoL(H <sub>2</sub> O)]Cl	+++	+++	+	–	++	–	+
[NiL(H <sub>2</sub> O)]Cl	–	–	+	+	–	++	–
[CuL(H <sub>2</sub> O)]Cl	+++	+	++	+++	+	+++	++
[ZnL(H <sub>2</sub> O)]Cl	–	++	++	–	+	++	–
<i>Amikacin</i>	+++	+++	+++	+++			
<i>Ciprofloxacin</i>	+++	+++	+++	+++			
<i>Ofloxacin</i>	+++	+++	+++	+++			
<i>Nystatin</i>					+++	+++	+++

The inhibition values: + denotes “less active” (0.1–0.5 cm beyond control); ++ denotes “moderate active” (0.6–1.0 cm beyond control); and +++ denotes “highly active” (1.1–1.5 cm beyond control).

Ni(II) complex does not exhibit well-defined crystalline peaks indicating that the complex is amorphous, while Co(II), Cu(II), and Zn(II) complexes show sharp peaks indicating their crystalline nature. However, single crystals of the complexes could not be obtained. The average crystallite sizes of the complexes  $d_{XRD}$  were calculated using Scherrer's formula [37]. The Co(II), Cu(II), and Zn(II) complexes have an average crystallite size of 29, 20, and 39 nm, respectively, suggesting that the complexes are nanocrystalline.

### 3.10. Scanning electron microscopy

The SEM micrographs of the complexes are given in Supplementary material. The surface morphology of Ni(II) is quite different from Co(II), Cu(II), and Zn(II) complexes, clearly indicating that Ni(II) complex is amorphous, in agreement with the powder XRD results. The SEM images of Co(II), Cu(II), and Zn(II) complexes exhibit similar type morphology, but their particle sizes are different. The particle size of Cu(II) complex is smaller than Co(II) and Zn(II) complexes and the particles are glassy in nature.

### 3.11. Antimicrobial activity

The antimicrobial activities are summarized in table 5. The standard error (SE) for the experiment is  $\pm 0.001$  cm and the experiment is repeated three times under similar conditions. DMSO is used as negative control and *Amikacin*, *Ofloxacin*, and *Ciprofloxacin* were used as positive standards for antibacterial and *Nystatin* for antifungal activities.

The Schiff base and Zn(II) complex have reduced activity against most of the microbes. Co(II) complex was effective against *E. coli* and *B. subtilis* with inhibitory zone of 1.0–1.2 cm, Ni(II) complex has moderate activity toward the fungal species *A. flavus* whereas higher antimicrobial activity has been exhibited by Cu(II) complex for *E. coli*, *S. aureus*, *A. flavus* and moderate activity toward *C. albicans* and *P. aeruginosa*. The reduced antimicrobial activity of Zn(II) complex may be due to poor solubility.

Antimicrobial activity of all complexes at low concentration toward the microbes is very low. The activity of the Schiff-base ligand and its complexes increases with the increase in concentration because the concentration plays a vital role in increasing the degree of inhibition. The antimicrobial activity also depends on the size of the particle, because nanosized particles exhibit increasing antimicrobial activity [38]. Further, the activities with respect to ligand and metal complexes follow the order ligand < Zn(II) < Co(II) < Ni(II) < Cu(II), similar to those seen in earlier reports [39].

### 3.12. Nuclease activity

Gel electrophoresis experiments using CT DNA were performed with the ligand and its complexes in the presence and absence of H<sub>2</sub>O<sub>2</sub> as oxidant. The nuclease activity of the complexes was also investigated in the presence of a free radical scavenger DMSO. The Cu(II) complex cleaves DNA more efficiently in the presence of an oxidant than the ligand, Co(II) and Ni(II) complexes (Supplementary material). The complexes cleave DNA into smaller fragments, but in lane 4 Cu(II) complex degrades DNA completely so that there is no band observed. This may be attributed to formation of hydroxyl-free radicals. The production of a hydroxyl radical [40] due to the reaction between the Cu(II) complex and oxidant may be explained as shown below:



These OH-free radicals participate in oxidation of the deoxyribose moiety, followed by hydrolytic cleavage of the sugar phosphate backbone [41]. The more pronounced nuclease activity of these adducts in the presence of oxidant as compared to the parent complexes can be due to the increased production of hydroxyl radicals. The nuclease activity of the complexes has also been investigated in the presence of a free radical scavenger DMSO, which diminishes the nuclease activity of the complexes, indicating involvement of the hydroxyl radical in the cleavage process.

## 4. Conclusion

The Co(II), Ni(II), Cu(II), and Zn(II) Schiff-base complexes of cuminaldehyde-L-histidine were prepared and characterized using different analytical techniques. The Schiff-base ligand is tridentate, coordinating through azomethine nitrogen, imidazole nitrogen, and carboxylato oxygen. The electronic spectral data and magnetic measurements suggest that Co(II) and Ni(II) complexes are tetrahedral, while Cu(II) complex has distorted square planar geometry. ESR spectrum of Cu(II) complex also reveals that it is distorted. TG/DTA analysis indicates the presence of coordinated water molecule in the complexes. The antimicrobial and CT-DNA cleavage studies reveal that the complexes show higher activity than the ligand.

## References

- [1] P. Deschamps, P.P. Kulkarni, B. Sarkar. *Inorg. Chem.*, **42**, 7366 (2003).
- [2] P.K. Sasmal, A.K. Patra, M. Nethaji, A.R. Chakravarty. *Inorg. Chem.*, **46**, 11112 (2007).

- [3] I. Sakiyan, E. Logoglu, S. Arglan, N. Sari, N. Sakiyan. *Biometals*, **17**, 115 (2004).
- [4] C.M. Alvarez, R.G. Rodriguez, D. Miguel. *J. Organomet. Chem.*, **692**, 5717 (2007).
- [5] H. Bian, F. Huang, X. Yang, O. Ya, A. Liang. *J. Coord. Chem.*, **61**, 802 (2008).
- [6] M. Nath, R. Yadov. *Bull. Chem. Soc. Japan*, **70**, 131 (1997).
- [7] D. Sattari, E. Alipour, S. Shirani, J. Amighian. *J. Inorg. Biochem.*, **45**, 115 (1992).
- [8] B. Macias, M.V. Villa, B. Gomez, J. Borrás. *J. Inorg. Biochem.*, **101**, 444 (2007).
- [9] E. Aeronoff-spencer, C.S. Burns, N.I. Ardierich, G.J.B. Gerfen, G.L. Millhauser. *Biochemistry*, **39**, 13760 (2000).
- [10] M.S. Nair, C.R.S. Raj. *J. Coord. Chem.*, **62**, 2903 (2009).
- [11] T. Nitoda, M.D. Fan, I. Kubo. *Phytother. Res.*, **22**, 809 (2008).
- [12] T. Sekine, M. Sugano, A. Majid, Y. Fujii. *J. Chem. Ecol.*, **33**, 2123 (2007).
- [13] K. Nihei, Y. Yamagiwa, T. Kamikawa, I. Kubo. *Bioorg. Med. Chem. Lett.*, **14**, 681 (2004).
- [14] A.G. Quiroga, J.M. Perez, I. Lopez-Solera, J.R. Masague, A. Luque, P. Roman, A. Edwards, C. Alonso, C. Navarro-Ranninger. *J. Med. Chem.*, **41**, 1399 (1998).
- [15] J.M. Perez, A.I. Matesanz, A.M. Ambite, P. Navarro, C. Alonso, P. Souza. *J. Inorg. Biochem.*, **75**, 255 (1999).
- [16] A.G. Quiroga, J.M. Perez, E.I. Montero, D.X. West, C. Alonso, C.N. Ranninger. *J. Inorg. Biochem.*, **75**, 293 (1999).
- [17] P.M. Krishna, K.H. Reddy, J.P. Pandey, D. Siddavattam. *Transition Met. Chem.*, **33**, 661 (2008).
- [18] A.I. Vogel. *A Textbook of Quantitative Inorganic Analysis Including Elementary Instrumental Analysis*, 4th Edn, p. 91, Longman, London (1978).
- [19] A.W. Bauer, W.M.M. Kirby, J.C. Sherries, M. Truck. *Am. J. Clin. Pathol.*, **45**, 493 (1996).
- [20] J.C. Pessoa, M.T. Duarte, R.D. Gillard, C. Madeira, P.M. Matias, I. Tomaz. *J. Chem. Soc., Dalton Trans.*, 4015 (1998).
- [21] K. Nakamoto. *Infra-red and Raman Spectra of Inorganic and Coordination Compounds*, 3rd Edn, p. 112, John Wiley & Sons, New York (1978).
- [22] J.J.P. Stewart. *J. Comput. Chem.*, **12**, 320 (1991).
- [23] M.M. Taguikhan, N.H. Khan, R.I. Kureshy. *Tetrahedron: Asymmetry*, **3**, 307 (1992).
- [24] G.B. Deacon, R.J. Phillips. *Coord. Chem. Rev.*, **33**, 227 (1980).
- [25] W.M. Hosny. *Synth. React. Inorg. Met.-Org. Chem.*, **28**, 1029 (1998).
- [26] A.B.P. Lever. *Inorganic Electronic Spectroscopy*, 2nd Edn, Elsevier, New York (1984).
- [27] R.N. Patel. *Indian J. Chem.*, **48A**, 173 (2009).
- [28] M.R. Wagner, F.A. Walker. *Inorg. Chem.*, **22**, 3021 (1983).
- [29] M. Nath, P. Arora. *Synth. React. Inorg. Met.-Org. Chem.*, **23**, 1523 (1993).
- [30] A.A. Osowole, G.A. Kolawole, O.E. Fagade. *Synth. React. Inorg. Met.-Org. Chem.*, **35**, 829 (2005).
- [31] T.B.S.A. Ravooof, K.A. Crouse, I.M. Tahir, A.R. Cowley, A. Ali. *Polyhedron*, **26**, 1159 (2007).
- [32] D. Kivelson, R. Neiman. *J. Chem. Phys.*, **35**, 149 (1961).
- [33] G. Speie, J. Csihony, A.M. Whalen, C.G. Pie. *Inorg. Chem.*, **35**, 3519 (1996).
- [34] S.M. Mamdoush, S.M. Abou, S.M. Elenein, H.M. Kamel. *Indian J. Chem.*, **41A**, 297 (2002).
- [35] B.J. Hathaway, G.A.A. Tomlinson. *Coord. Chem. Rev.*, **5**, 1 (1970).
- [36] A. Raman, A. Kulandaisamy, C. Thangaraja. *Transition Met. Chem.*, **28**, 29 (2003).
- [37] C.J. Dhanaraj, M.S. Nair. *Eur. Polym. J.*, **45**, 565 (2009).
- [38] G.V. Nazarov, S.E. Galan, E.V. Nazarova, N.N. Karkishchenko, M.M. Muradov, V.A. Stepanov. *Pharm. Chem. J.*, **43**, 163 (2009).
- [39] G.B. Bagihalli, S.A. Patil. *J. Coord. Chem.*, **62**, 1690 (2009).
- [40] K. Yamamoto, S. Kawanishi. *J. Biol. Chem.*, **15**, 264 (1984).
- [41] P. Merfey, E.R. Robinson. *Mutat. Res.*, **86**, 155 (1981).